

Received: November 11, 1978

SOLID-GAS REACTIONS OF DIPHENYL-F-PHENYL PHOSPHINE OXIDE WITH METHYLAMINE
AND AMMONIA [1]

DOUGLAS G. NAAE* and TSUNG-WHEI LIN

Department of Chemistry, University of Kentucky
Lexington, Kentucky 40506 (U.S.A.)

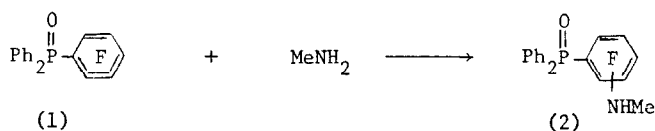
SUMMARY

The reactions of gaseous MeNH_2 and NH_3 with solid $\text{Ph}_2\text{P}(\text{O})\text{C}_6\text{F}_5$ have been examined. The principal products of the reaction are para- $\text{Ph}_2\text{P}(\text{O})\text{C}_6\text{F}_4\text{NHMe}$ and para- $\text{Ph}_2\text{P}(\text{O})\text{C}_6\text{F}_4\text{NH}_2$ and not the ortho isomers. This is due to the low reactivity of $\text{Ph}_2\text{P}(\text{O})\text{C}_6\text{F}_5$ and the nature of the solid-gas reaction. This reactivity is contrasted with the prediction based on the X-ray crystal structure of $\text{Ph}_2\text{P}(\text{O})\text{C}_6\text{F}_5$, which has been determined. The solution reactivity of $\text{Ph}_2\text{P}(\text{O})\text{C}_6\text{F}_5$ is compared to $\text{C}_6\text{F}_5\text{NO}_2$.

INTRODUCTION

Nucleophilic substitution in polyfluorinated aromatic compounds is a well known reaction [2]. The usual course of the reaction is for substitution to occur para to the substituent on a pentafluorophenyl ring. There are, however, a number of substituents which give rise to substantial amounts of ortho substitution under certain conditions: $-\text{NO}_2$ [3,4]; $-\text{NO}$ [5]; $-\text{CO}_2\text{H}$ [6]; $-\text{CHO}$ [7]; and $-\text{P}(\text{O})\text{Ph}_2$ [8].

Previously we have reported that the reaction between solid, diphenyl-pentafluorophenyl phosphine oxide, (1), and gaseous methylamine, MeNH_2 , led to almost exclusive formation of the para-substituted product, (2), [1]. Ortho-(2) is the predominant product in benzene solution, and in ethanol solution para-(2) is the major product. Apparently, the large amount of



	<u>ortho</u>	<u>para</u>
benzene solution	94%	6%
ethanol solution	5	95
solid-gas	< 2	> 98

ortho substitution in benzene is caused by hydrogen bond formation between the amine and the oxygen of (1) [3,4,8]. Ethanol as the solvent prevents the amine from forming the hydrogen bond and normal para-substitution occurs instead.

The solid-gas reaction is intriguing because of the suppression of ortho-substitution and because of the physical nature of the reaction. When a powdered sample of (1) (or single crystals) is exposed to excess MeNH_2 , the color of (1) changes immediately from white to light yellow. After a short period the solid appears deliquescent and within 15 minutes the solid forms a melt (liquid phase) consisting of (1), (2), MeNH_2 , and $\text{MeNH}_3^+ \text{HF}_2^-$. The melt gradually solidifies and GLC analysis reveals that the product is > 98% para-(2).

An increase in the reaction temperature to 55°C and reduction of the amount of MeNH_2 to less than an equivalent amount prevents the formation of an observable melt during the solid-gas reaction. The reaction rate is quite slow with powdered (1) and after one week only a 5% yield of para-(2) is found. Ortho-(2) cannot be detected by GLC analysis. With single crystals of (1) no reaction is detected either visually or by GLC analysis.

In order to account for the predominance of para-(2) in the solid-gas reaction the crystal structure of (1) has been determined by x-ray crystallography, and the effect of solvent and stoichiometry on the reaction of (1) with MeNH_2 has been examined.

RESULTS AND DISCUSSION

Crystal Structure of (1)

The numbering scheme of the atoms is shown in Figure 1. As the space group is $\text{P } 2_1/\text{C}$ and there are eight molecules in the unit cell, there are two molecules in the asymmetric unit of the structure. The two molecules

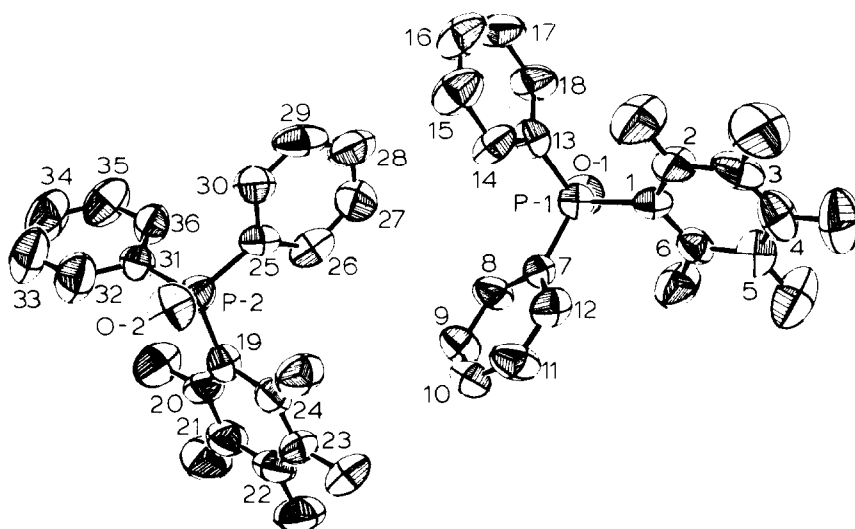


Fig. 1. View of the asymmetric unit of (1), hydrogen atoms have been omitted for clarity. Fluorine and hydrogen atoms are given the same number as the carbon to which they are bonded.

in the asymmetric unit have different conformations due to the rotation of the aromatic rings about the P-C bonds.

The average P-O bond length of 1.474 Å compares well with the distance of 1.46 Å reported for the P-O bond in triphenylphosphine oxide, Ph_3PO [9]. In Ph_3PO an average P-C bond length of 1.76 Å was reported which is slightly shorter than the mean distance of 1.796 Å observed in (1). The mean C-C distance in the fluorinated rings is 1.370 Å and in the hydrocarbon rings 1.378 Å. These distances are slightly shorter than the mean C-C distance of 1.40 Å in Ph_3PO . This trend of C-C bonds in fluorinated systems being slightly shorter than in the parent hydrocarbon has been noted previously [10].

The C-F distances in (1) range from 1.319 to 1.350 Å, with a mean of 1.337 Å. These values are slightly shorter than the mean value in 2,3,4,5,6-pentafluorobiphenyl (1.347 Å) [11], 2,3,5,6-tetrafluorobiphenyl (1.360 Å) [12], and F-biphenyl (1.344 Å) [13]. Part of this discrepancy may be due to the bond distances in (1) not being corrected for thermal motion.

The molecular packing of Ph_3PO in the solid is characterized by stacks of molecules parallel to \vec{c} . The individual molecules within each stack are oriented so a vector from P to O is approximately parallel to the direction of the stack. Thus, the P-O dipoles are aligned within the stack.

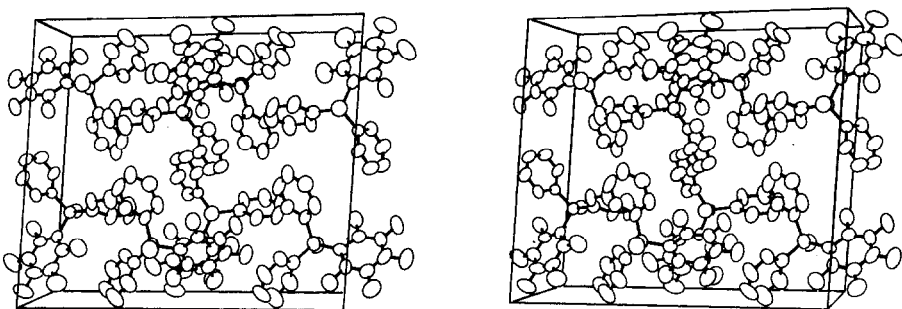


Fig. 2. Stereoscopic view of the unit cell of (1), hydrogen atoms have been omitted for clarity. The \vec{a} axis is vertical, the \vec{c} axis is horizontal, and the \vec{b} axis points out of the paper.

The molecular packing of (1) is shown in Figure 2. As can be seen (1) also forms stacks of molecules parallel to \vec{c} . However, in (1) the P-O vectors are directed parallel to \vec{b} (perpendicular to the stack direction).

There are no apparent intermolecular contacts or interactions between the pentafluorophenyl rings and the phenyl rings as occur in the crystal structures 2,3,4,5,6-pentafluorobiphenyl [1,11], 2,3,5,6-tetrafluorobiphenyl [12], and the molecular complexes between F-biphenyl and biphenyl or 4-bromobiphenyl [14]. These crystal structures are characterized by stacks of aromatic rings where fluorinated and non-fluorinated rings alternate within the stacks. This type of interaction is absent in (1). The reactivity of (1) with gaseous MeNH_2 is consistent with the molecular packing of the compound. A melt is readily formed during the reaction. The biphenyl derivatives and complexes exhibit a greatly reduced reactivity due to their molecular packing [1,14].

The nature of the molecular packing of (1) results in the oxygen of each molecule being in a position that should be accessible to a MeNH_2 molecule entering the crystal lattice. In addition, the ortho and para carbons of the C_6F_5 ring appear equally accessible. Thus, the prediction of reactivity based on the molecular packing is that a substantial amount of ortho substitution should occur. The lack of ortho substitution is indicative of the reaction not being under control of the crystal lattice.

Reaction of (1) with MeNH_2

In the presence of excess MeNH_2 solid (1) is readily converted to para-(2) with less than 2% ortho-(2) being formed. The physical state of the reaction involves the formation of a melt in which a substantial portion of the reaction occurs. (The melt is indicative of reaction as exposure of solid para-(2) to excess MeNH_2 does not lead to the formation of a melt). The melt contains excess MeNH_2 and should be similar to the solution reaction in ethanol where hydrogen bonding between the amine and the phosphine oxide is prevented. This suggests that the concentration of MeNH_2 in a solution reaction should change the ortho/para product ratio.

Table I lists the results of the effect of solvent and MeNH_2 concentration on the formation of (2). For comparison the reactions with $\text{C}_6\text{F}_5\text{NO}_2$ are given. As is evident, the ortho/para ratio for (1) is quite dependent upon the solvent composition. Even small additions of ethanol to the reaction mixture have a pronounced effect. The presence of excess MeNH_2 causes a significant decrease in the ortho/para ratio. This is probably due to aggregation of MeNH_2 molecules about the oxygen of (1). This prevents subsequent MeNH_2 molecules from hydrogen-bonding to the oxygen and para substitution results.

Extrapolation of this trend to the solid-gas reaction of (1) with excess MeNH_2 leads to para-(2) becoming the predominant product as the reaction medium is now the amine. The implication for the reaction of solid (1) with an equivalent of MeNH_2 (where a visible melt is not formed) is that considerable aggregation of MeNH_2 molecules is occurring about the phosphine oxide moiety which precludes formation of ortho-(2).

The reactions of $\text{C}_6\text{F}_5\text{NO}_2$ show the same trends as (1). However, because $\text{C}_6\text{F}_5\text{NO}_2$ is considerably more reactive than (1) toward MeNH_2 , the trends are suppressed, as ortho substitution is the major process even in ethanol. This trend of reactivities is in agreement with ortho substitution having a greater activation energy than para substitution [15]. Thus, (1) exhibits a pronounced medium effect because of its low reactivity, while $\text{C}_6\text{F}_5\text{NO}_2$ has less distinction between ortho and para substitution because of its greater reactivity.

X-Ray powder pattern analysis of the reaction of solid (1) with an equivalent of MeNH_2 shows only the diffraction pattern of (1). For powdered samples exposed to an excess of MeNH_2 only the diffraction pattern of para-(2) is found. The by-product of the solid-gas reaction appears to

TABLE I Effect of solvent and amine concentration on product ratio

$$\text{X}-\text{C}_6\text{H}_4\text{F} + \text{MeNH}_2 \longrightarrow \text{X}-\text{C}_6\text{H}_4\text{NMe} + \text{HF}$$

ortho: *para*^a

Ratio $\text{MeNH}_2/\text{XC}_6\text{F}_5$	Solvent	$\text{X} = \text{Ph}_2\text{P}(\text{O})-$ ^b	$\text{X} = \text{O}_2\text{N}-$ ^c
1	C_6H_6	94:6 ^d	97:3
1	C_6H_6 , 7% $\text{C}_2\text{H}_5\text{OH}$	59:41	81:19
1	C_6H_6 , 14% $\text{C}_2\text{H}_5\text{OH}$	42:58	---
1	C_6H_6 , 41% $(\text{C}_2\text{H}_5)_2\text{O}$	84:16	89:11
1	C_6H_6 , 7% $(\text{CH}_3)_2\text{SO}$	38:62	79:21
6	C_6H_6	84:16	83:17
16	C_6H_6	75:25	---
1	$\text{C}_2\text{H}_5\text{OH}$	5:95	68:32 ^e

- a. procedures are given in the experimental section; the ratios have been normalized; for each compound only mono-substitution occurred.
- b. reaction temperature = 50°C.
- c. reaction temperature = 22°C (room).
- d. literature value = 82:18 (solvent = C_6H_6 , 2% $\text{C}_2\text{H}_5\text{OH}$), ref [8].
- e. literature value = 65:35, ref [3].

be $\text{MeNH}_3^+ \text{HF}_2^-$. This conclusion is based on the elemental analysis, Table II, of the material from the solid-gas reaction. The data in Table II also shows a loss of $\text{MeNH}_3^+ \text{HF}_2^-$ on standing. Apparently dissociation to MeNH_2 and HF occurs and these diffuse out of the solid.

Reaction of (1) with NH_3

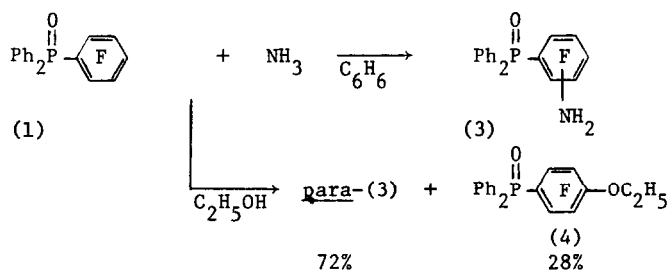
In solution, (1) is much less reactive toward NH_3 than MeNH_2 because NH_3 is a weaker nucleophile. In benzene at 50°C, with an equivalent of NH_3 , the major product, 89%, is the *para*-substituted isomer, *para*-(3). *Ortho*-(3) is formed only in 11% yield. This decrease in the *ortho/para* ratio, caused by a decrease in nucleophilicity, compliments the increase in the *ortho/para* ratio, caused by an increase in reactivity, for $\text{C}_6\text{F}_5\text{NO}_2$ (Table I).

TABLE II Quantitative elemental analysis of the product from the solid-gas reaction of (1) with MeNH₂^a

	% C	% H	% N
Sample A ^b	55.95	4.35	4.94
	56.11	4.39	5.11
Sample B	53.30	4.99	5.62
	53.54	4.98	5.81
Calculated:			
C ₁₉ H ₁₄ F ₄ NOP	60.16	3.69	3.69
C ₁₉ H ₁₄ F ₄ NOP + .55(CH ₃ NH ₃ ⁺ HF ₂ ⁻)	56.12	4.27	5.19
C ₁₉ H ₁₄ F ₄ NOP + 1.0(CH ₃ NH ₃ ⁺ HF ₂ ⁻)	53.33	4.67	6.22
C ₁₉ H ₁₄ F ₄ NOP + .50(CH ₃ NH ₃ ⁺ F ⁻)	57.85	4.20	5.19
C ₁₉ H ₁₄ F ₄ NOP + 1.0(CH ₃ NH ₃ ⁺ F ⁻)	55.81	4.65	6.51

a. details are given in the experimental section

b. sample A was allowed to stand ten days longer than sample B prior to analysis



Due to its lower nucleophilicity, the reaction of NH₃ with (1) is slower than the reaction of MeNH₂ with (1). The result is that for the reaction of NH₃ with (1) in ethanol, the attack by ethoxide (formed in situ by proton transfer to NH₃) on (1) to form (4) becomes appreciable.

The reaction of solid (1) with NH₃ gas is similar to the MeNH₂ reactions. When an excess of NH₃ is used, a melt is formed and reaction occurs in this liquid phase. When an equivalent or less of NH₃ is used and the reaction temperature is ca. 55°C the color of powdered (1) slowly changes from white to light yellow. Formation of a melt is not observed during the reaction, and only a 3% yield of *para*-(3) is found after one week. *Ortho*-(3) cannot be detected by GLC analysis. Single crystals of (1) do not appear to react with the gas.

EXPERIMENTAL

Melting points were recorded on a microscope hot stage and are uncorrected. ^{19}F NMR spectra were obtained on a Varian HA-60-IL spectrometer operated at 56.4 MHz, chemical shifts were measured relative to external C_6F_6 and were converted to δ^* values. Mass spectra were obtained on a Hitachi-Perkin-Elmer RMU-7 double focusing spectrometer. X-Ray powder patterns were recorded on conventional cameras with $\text{Cu K}\alpha$ radiation. Quantitative elemental microanalysis were performed by Galbraith Laboratories, Inc., Knoxville, Tennessee. GLC Analyses were performed on a Varian 920 gas chromatograph, a 5-ft, 2% OV-101 column was used. A Wild M-7 trinocular polarizing microscope was used for the microscopic examination of single crystals and for the observation of the solid-gas reactions.

The reported procedure [16] was used for the preparation of $\text{Ph}_2\text{PC}_6\text{F}_5$ which was converted to $\text{Ph}_2\text{P}(\text{O})\text{C}_6\text{F}_5$, (1), by oxidation with hydrogen peroxide [8]. Samples of ortho- and para- $\text{Ph}_2\text{P}(\text{O})\text{C}_6\text{F}_4\text{NHMe}$, (2), were prepared by the reported procedure [8].

Reaction of Solid $\text{Ph}_2\text{P}(\text{O})\text{C}_6\text{F}_5$, (1), with MeNH_2 gas

(a) Excess amine

A weighed sample of (1) (crystals from hexane or powdered crystals) was placed in a glass chamber which was flushed with dry nitrogen. A slow stream of dry MeNH_2 gas was passed over the solid for ca. 20 seconds. The chamber was sealed and the change in physical appearance followed by microscopic examination. Single crystals, which were initially clear, quickly turned opaque. Tiny liquid pools, which appeared on the surface of the crystals, slowly merged and then recrystallized. GLC Analysis revealed no unreacted (1) and > 98% para-(2) and < 2% ortho-(2).

(b) Limited amine

Powdered $\text{Ph}_2\text{P}(\text{O})\text{C}_6\text{F}_5$ (3.8 mg, 0.010 mmole) was placed in the reaction chamber and the chamber flushed with dry nitrogen. Then 0.13 mL (0.006 mmole) of gaseous MeNH_2 was added via syringe. The reaction chamber was then placed on a hot plate set at 55°C . The solid gradually changed from white to a light yellow, but a melt was not observed by microscopic examination. After one week, GLC Analysis showed a 5% yield of para-(2) while ortho-(2) was not detected.

Crystal Structure Determination of $\text{Ph}_2\text{P}(\text{O})\text{C}_6\text{F}_5$, (1)

Colorless elongated plates were obtained by crystallization from n-hexane. Preliminary examination on a Weissenberg camera revealed monoclinic diffraction symmetry with systematic extinctions for $0k0$ ($k = \text{odd}$) and $h0l$ ($l = \text{odd}$) which is consistent with the space group $\text{P}2_1/\text{C}$. A density of 1.47 g cm^{-3} was measured by flotation in aqueous ZnCl_2 .

Intensity data for a crystal of dimensions $0.37 \times 0.25 \times 0.06 \text{ mm}$ mounted in a glass capillary were obtained on an Enraf-Nonius CAD-4 diffractometer using monochromatic $\text{Mo K}\alpha$ X-rays ($\lambda = 0.7107 \text{ \AA}$). Fifteen computer centered reflections were used in a least squares routine to determine cell constants of $a = 17.069 (4) \text{ \AA}$, $b = 10.101 (3) \text{ \AA}$, $c = 18.972 (6) \text{ \AA}$ and $\beta = 94.28 (3)^\circ$. The calculated volume is $V = 3261.9 \text{ \AA}^3$, and for $Z = 8$ the calculated density is 1.50 g cm^{-3} . As $\text{P}2_1/\text{C}$ requires only $Z = 4$, there are 2 molecules of (1) in the asymmetric unit of the unit cell.

Intensity measurements were made for 3091 independent reflections with $\theta \leq 20.0^\circ$ using the $\theta - 2\theta$ scan technique with a variable scan rate. Moving-crystal moving-counter background counts were taken at each end of the scan range. The ratio of scan time to background time was 2.0. Three reflections were measured periodically as a check on crystal and electronic stability. No decrease in intensity of these standard reflections was observed during data collection.

A total of 1321 reflections had $I > 3 \sigma(I)$ where $\sigma(I) = S[\text{CT} + 4(B_1 + B_2)]^{1/2}$ and S is the scan speed, CT is the scan count, and B_1 and B_2 are the background counts. Lorentz and polarization corrections were applied to the data and normalized structure factors generated (E 's). A correction for absorption was not done ($\mu = 2.34 \text{ cm}^{-1}$).

Structure solution was by direct methods via MULTAN [17] with all 50 non-hydrogen atoms located on subsequent Fourier maps. Full-matrix least squares refinement of positions and anisotropic temperature factors led to an agreement factor (defined below) of $R_1 = 0.062$. Scattering factors were obtained for the usual source [18]. The twenty hydrogen atoms were located in a difference Fourier map. However, they were placed at their theoretical positions and assigned an isotropic temperature factor of 5.0 and not refined during subsequent cycles. Final least squares refinement converged to the following values where $W = 4F_o^2/\sigma^2(F_o^2)$

$$R_1 = \Sigma ||F_o| - F_c| / \Sigma |F_o| = 0.044$$

$$R_2 = [\Sigma w(|F_o| - |F_c|)^2 / \Sigma w F_o^2]^{1/2} = 0.047$$

for 451 variable parameters. The error in an observation of unit weight was 1.25 and the maximum parameter shift in the final cycle was 0.2 times its esd.

Table III Fractional coordinates ($\times 10^4$) of (1) with estimated standard deviations in parentheses.

Atom	X	Y	Z	Atom	X	Y	Z
P1	3137.7 (15)	3374 (3)	44893 (13)	C32	9231 (10)	1732 (13)	3271 (7)
P2	7879.9 (17)	1626 (3)	3936.7 (14)	C33	9743 (10)	2247 (19)	2832 (10)
O1	3162 (3)	4826 (6)	4453 (3)	C34	9591 (11)	3367 (22)	2465 (8)
O2	7971 (4)	173 (7)	3991 (3)	C35	8885 (10)	4029 (12)	2530 (6)
C1	2222 (6)	2788 (12)	4810 (6)	C36	8351 (6)	3516 (13)	2976 (6)
C2	1708 (9)	1890 (14)	4498 (7)	F2	1834 (4)	1303 (7)	3895 (4)
C3	1018 (9)	1528 (14)	4792 (9)	F3	547 (5)	644 (9)	4461 (4)
C4	846 (8)	2070 (16)	5419 (11)	F4	182 (4)	1706 (8)	5701 (4)
C5	1338 (10)	2945 (13)	5748 (7)	F5	1164 (4)	3446 (8)	6372 (4)
C6	2008 (7)	3305 (12)	5440 (7)	F6	2482 (4)	4149 (6)	5803 (3)
C7	3882 (6)	2665 (10)	5082 (5)	F20	9140 (4)	3774 (6)	4534 (3)
C8	4597 (7)	3308 (11)	5133 (5)	F21	9281 (4)	4785 (7)	5807 (3)
C9	5229 (6)	2841 (12)	5550 (6)	F22	8310 (4)	4077 (7)	6795 (3)
C10	5142 (7)	1690 (14)	5928 (5)	F23	7189 (4)	2214 (7)	6483 (3)
C11	4449 (8)	1033 (11)	5895 (6)	F24	7024 (4)	1171 (7)	5198 (3)
C12	3805 (6)	1517 (12)	5476 (6)	H8	4670	4210	4830
C13	3234 (6)	2626 (10)	3647 (6)	H9	5780	3370	5580
C14	3576 (7)	1413 (12)	3571 (5)	H10	5640	1280	6250
C15	3642 (7)	868 (12)	2894 (8)	H11	4390	120	6190
C16	3381 (8)	1592 (16)	2314 (6)	H12	3250	1010	5470
C17	3045 (8)	2784 (14)	2378 (7)	H14	3790	880	4030
C18	2978 (7)	3327 (12)	3044 (7)	H15	3920	-80	2830
C19	8061 (8)	2402 (11)	4787 (6)	H16	3440	1190	1790
C20	8623 (8)	3309 (15)	4978 (7)	H17	2840	3320	1910
C21	8739 (8)	3884 (13)	5642 (9)	H18	2720	4320	3090
C22	8259 (10)	3523 (15)	6141 (8)	H26	6720	3720	4370
C23	7684 (9)	2581 (15)	6008 (8)	H27	5420	4350	3800
C24	7605 (7)	2061 (13)	5338 (8)	H28	4860	3150	2760
C25	6916 (6)	2184 (12)	3624 (6)	H29	5620	1430	2240
C26	6492 (8)	3208 (12)	3909 (5)	H30	6890	710	2810
C27	5763 (8)	3564 (13)	3593 (7)	H32	9370	820	3550
C28	5452 (8)	2895 (17)	3005 (8)	H33	11310	1770	2780
C29	5853 (10)	1909 (16)	2716 (6)	H34	9980	3770	2110
C30	6584 (8)	1544 (12)	3030 (7)	H35	8730	4910	2220
C31	8529 (7)	2371 (12)	3353 (5)	H36	7800	4020	3030

The final difference Fourier map showed no residual electron density as high as a hydrogen atom on a previous difference map. Final fractional coordinates and anisotropic temperature factors for all atoms are collated in Tables III and IV, respectively.

Solvent and Concentration Study for MeNH₂ Reactions

In a small flask were placed Ph₂P(O)C₆F₅, (1), (25 mg, 0.068 mmole) and 0.6 mL solvent, followed by 0.136 mL (0.068 mmole) of a 0.5 molar solution of MeNH₂ in benzene. The solution was heated to 50°C and allowed to react overnight. The results of various runs are given in Table I.

The reactions with C₆F₅NO₂ were also performed as described above but the reaction temperature was room temperature and reaction times were five minutes or less.

Elemental Analysis of the Solid-Gas Reaction

Two complete reactions of powdered (1) with excess MeNH₂ gas were performed. The first was found by GLC analysis to be complete after 7 days. No unreacted (1) was observed. The remaining material (Sample A) was stored without additional handling or manipulation.

A second reaction identical to the first was then started. After 10 days, GLC analysis showed no unreacted (1). The remaining sample (B) and sample A were submitted for quantitative analysis and the results are listed in Table II.

Preparation of (4-amino-2,3,5,6-tetrafluoro)phenyldiphenylphosphine oxide; para-(3) (nc)

Ammonia (28 mmole, 0.6 mL) was condensed in a glass ampoule, followed by addition of Ph₂P(O)C₆F₅, (1), (0.54 mmole, 0.2 g) and 11 mL of benzene. ~~The ampoule was sealed and heated at 69°C for 7 days. The ampoule was~~ opened and the solvent removed. GLC Analysis showed that the solid residue was > 99% one product, no unreacted (1) was found. The material was recrystallized from benzene to give 0.15 g (75% yield) of para-(3), m.p. = 209-210°C. The structure was assigned by ¹⁹F nmr, multiplets of equal intensity at δ^* = 132.7 and 161.5 ppm. Mass spectrometry showed M⁺ at 365 m/e. Elemental analysis: Found: C, 59.00; H, 3.34. C₁₈H₁₂F₄NO⁺ requires: C, 59.18; H, 3.28.

Table IV Anisotropic temperature factors ($\times 10^4$) of the form:
 $\exp[-(\beta_{11}h^2 + \beta_{22}k^2 + \beta_{33}l^2 + 2\beta_{12}hk + 2\beta_{13}hl + 2\beta_{23}kl)]$.

Atom	B11	B22	B33	B12	B13	B23
P1	45.2 (14)	106 (4)	33.8 (11)	-4.2 (22)	1.4 (10)	-0.7 (20)
P2	59.8 (17)	123 (4)	35.7 (12)	-2.6 (25)	7.8 (11)	0.8 (22)
O1	61 (4)	80 (10)	49 (3)	-4 (4)	3.4 (24)	1 (4)
O2	84 (5)	94 (10)	57 (3)	8 (5)	10 (3)	1 (5)
C1	51 (6)	117 (16)	26 (4)	-2 (8)	-7 (5)	-7 (7)
C2	64 (7)	183 (21)	37 (5)	-34 (11)	-1 (6)	-30 (9)
C3	50 (8)	184 (20)	56 (7)	-44 (11)	-13 (6)	-2 (11)
C4	39 (7)	177 (23)	70 (8)	-22 (11)	7 (6)	18 (11)
C5	59 (8)	108 (18)	57 (7)	-1 (10)	10 (7)	-2 (9)
C6	38 (6)	147 (17)	46 (6)	-24 (9)	-4 (5)	3 (10)
C7	40 (5)	105 (14)	24 (4)	-11 (7)	2 (4)	1 (6)
C8	48 (5)	157 (16)	40 (4)	6 (10)	-2 (4)	17 (8)
C9	43 (6)	161 (19)	55 (5)	-8 (9)	-2 (5)	10 (8)
C10	55 (6)	158 (17)	40 (5)	6 (10)	-6 (4)	5 (8)
C11	60 (7)	161 (18)	51 (5)	-12 (10)	-7 (5)	35 (8)
C12	60 (6)	129 (17)	36 (4)	-24 (9)	3 (4)	15 (7)
C13	48 (5)	83 (14)	42 (5)	14 (7)	3 (4)	13 (7)
C14	88 (7)	140 (20)	27 (4)	37 (9)	6 (4)	6 (7)
C15	95 (8)	175 (19)	47 (6)	33 (10)	15 (5)	1 (10)
C16	103 (8)	180 (21)	41 (6)	28 (11)	12 (5)	-19 (10)
C17	115 (9)	188 (23)	27 (5)	40 (11)	-7 (5)	6 (8)
C18	86 (7)	134 (16)	39 (5)	22 (9)	-2 (5)	10 (9)
C19	42 (6)	121 (16)	41 (6)	-10 (8)	2 (5)	3 (8)
C20	56 (7)	202 (21)	26 (5)	7 (11)	3 (5)	15 (9)
C21	48 (7)	199 (24)	48 (7)	-19 (10)	0 (6)	12 (11)
C22	56 (7)	177 (22)	40 (6)	13 (10)	-14 (6)	-6 (10)
C23	58 (7)	209 (23)	30 (6)	18 (11)	11 (6)	30 (9)
C24	44 (6)	164 (19)	40 (6)	-7 (9)	-1 (5)	8 (9)
C25	51 (6)	128 (16)	28 (4)	-19 (8)	-4 (4)	5 (7)
C26	73 (7)	111 (16)	36 (4)	-12 (9)	9 (5)	-4 (7)
C27	50 (6)	257 (25)	52 (6)	26 (11)	2 (5)	24 (10)
C28	69 (7)	281 (28)	33 (5)	-23 (12)	-7 (5)	18 (10)
C29	89 (9)	205 (23)	34 (5)	-46 (13)	2 (6)	-3 (9)
C30	64 (7)	163 (17)	43 (5)	-13 (10)	-1 (5)	6 (9)
C31	50 (6)	135 (17)	35 (5)	14 (8)	5 (4)	-11 (8)
C32	86 (8)	179 (19)	56 (6)	15 (12)	24 (6)	7 (10)
C33	84 (9)	280 (32)	72 (9)	20 (15)	28 (7)	-6 (12)
C34	85 (10)	365 (39)	59 (7)	-39 (17)	46 (7)	-8 (14)
C35	96 (8)	193 (20)	49 (5)	-36 (13)	31 (6)	13 (8)
C36	55 (6)	150 (19)	41 (5)	10 (9)	9 (4)	15 (7)
F2	105 (5)	287 (14)	58 (3)	-86 (6)	12 (3)	-51 (5)
F3	89 (5)	383 (17)	90 (4)	-109 (8)	-1 (3)	-25 (7)
F4	59 (3)	279 (12)	100 (4)	-26 (6)	29 (3)	23 (6)
F5	106 (5)	268 (13)	73 (3)	-36 (6)	47 (3)	-37 (6)
F6	76 (4)	243 (10)	45 (2)	-48 (5)	13 (2)	-33 (5)
F20	75 (4)	252 (12)	50 (3)	-56 (5)	15 (3)	-13 (4)
F21	81 (4)	240 (12)	64 (3)	-35 (6)	-11 (3)	-21 (5)
F22	103 (4)	289 (12)	39 (3)	23 (6)	-10 (3)	-16 (5)
F23	87 (4)	333 (14)	35 (2)	4 (6)	17 (2)	16 (5)
F24	76 (4)	228 (11)	44 (2)	-34 (6)	12 (2)	16 (4)

A small amount (< 1%) of a second product was observed by GLC Analysis. Because of its retention time it is thought to be ortho-(3).

Reaction of $\text{Ph}_2\text{P}(\text{O})\text{C}_6\text{F}_5$, (1), with NH_3 in Ethanol

A solution of $\text{Ph}_2\text{P}(\text{O})\text{C}_6\text{F}_5$ (1) (0.33 g, 0.9 mmole) in 10 mL absolute ethanol was combined with 0.35 mL (2.8 mmole) of a 15% w/v NH_3 /ethanol solution. The mixture was heated at ca. 60°C for three days. The solution was poured into water, extracted into $\text{CH}_2\text{Cl}_2/\text{CCl}_4$, dried (molecular sieves), and the solvent removed. GLC Analysis of the solid residue showed two products in the ratio of 28:72. The major product was identified as para-(3) by its GLC retention time and ^{19}F nmr. The minor product was identified as (4-ethoxy-2,3,5,6-tetrafluorophenyl)diphenylphosphine oxide, (4) by ^{19}F nmr (two multiplets of equal intensity at $\delta^* = 130.6$ and 155.7 ppm - indicative of para-substitution) and mass spectrometry, $\text{M}^+ = 394$ m/e. No attempt was made to separate the compounds.

ACKNOWLEDGEMENT

This research was partially supported by the Chemical Instrumentation Program, grant No. CHE 77-07445, of the National Science Foundation.

REFERENCES

- 1 Preliminary communication, T.W. Lin and D.G. Nae, Tetrahedron Lett., (1978) 1653.
- 2 for example, see R.D. Chambers, Fluorine in Organic Chemistry, Wiley and Sons, 1973, p. 261 ff.
- 3 J.G. Allen, J. Burdon, and J.C. Tatlow, J. Chem. Soc. (1965) 1045.
- 4 G.M. Brooke, J. Burdon, and J.C. Tatlow, *ibid.*, (1961) 802.
- 5 J. Burdon and D.F. Thomas, Tetrahedron, 21 (1965) 2389.
- 6 J. Burdon, W.G. Hollyhead, and J.C. Tatlow, J. Chem. Soc., (1965) 6336.
- 7 E.V. Aroskar, P.J.N. Brown, R.G. Plevy, and R. Stephens, *ibid.*, (1968) 1569.
- 8 J. Burdon, I.N. Rozhkov, and G.M. Perry, J. Chem. Soc. (C), (1969) 2615.
- 9 G. Bandoli, G. Bortolozzo, D.A. Clemente, U. Croatto, and C. Panattoni, J. Chem. Soc. (A), (1970) 2278.

- 10 M.J. Hamor and T.A. Hamor, *Acta Crystallogr.*, B32, (1976) 2475.
- 11 C.P. Brock, D.G. Naeae, N. Goodhand, and T.A. Hamor, *ibid.*, B, in press.
- 12 N. Goodhand and T. Hamor, *ibid.*, B34, (1978) 1644.
- 13 W.B. Gleason and D. Britton, *Cryst. Struct. Comm.*, 5, (1976) 483.
- 14 S.L. Pirtle and D.G. Naeae, to be published.
- 15 J. Burdon and I.W. Parsons, *J. Amer. Chem. Soc.*, 99, (1977), 7445.
- 16 R.D.W. Kemmitt, D.I. Nichols, and R.D. Peacock, *J. Chem. Soc. (A)*, (1968) 2149.
- 17 G. Germain, P. Main, and M.M. Woolfson, *Acta Crystallogr, Sect A*, 27 (1971) 368.
- 18 D.T. Cromer and J.T. Waber, "International Tables for X-Ray Crystallography," Vol IV, Kynoch Press, Birmingham, England, (1974) Table 2.2B.